A Movable Thomson Scattering System Based on Optical Fibers (TS-Probe)

Kazumichi NARIHARA and Hiroshi HAYASHI

National Institute for Fusion Science, 322-6 Oroshi-cho, Toki 509-5292, Japan

This paper proposes a movable compact Thomson scattering (TS) system based on optical fibers (TS-probe). The TS-probe consists of a probe head, optical fibers, a laser diode, a polychromator, and lock-in amplifiers. Laser beam optics and light collection optics are mounted rigidly on a probe head with a fixed scattering position. Laser light and scattered light are transmitted by flexible optical fibers, enabling us to move the TS-probe head freely during plasma discharge. The light signal scattered from an amplitude-modulated laser is detected against the plasma light based on the principle of the lock-in amplifier. With a modulated laser power of 300 W, the scattered signal from a sheet plasma 15 mm deep with $n_e \sim 10^{19} \, \text{m}^{-3}$ can be measured with 10 % accuracy by setting the integrating time to 0.1 s. The TS-probe head is similar to a 1/20 model of the currently operating Large Helical Device-TS.

1. Introduction

In fusion-oriented plasma experiments, Thomson scattering (TS) is a standard method of obtaining electron temperature (T_e) and density (n_e) profile data. Its advantage is that it gives local values of T_e and n_e with high confidence and accuracy. There are, however, disadvantages; the small probability of TS ($n_e \sigma L < 10^{-11}$) necessitates bright optics and highly efficient detectors even with currently available high-energy pulse lasers, and precise laser beam alignment is often required. As a result, TS typically is costly and requires a tedious labor in construction and maintenance, preventing its easy use at various locations in a plasma confinement device. As a possible solution, this paper proposes the concept of a TS-probe that is compact and can be moved, like a Langmuir probe, to a desired position around a plasma without requiring laser beam alignment. We proposed a similar idea 13 years ago [1], but it has not yet been realized because a suitable light source had not been available. Recently developed laser diodes that can deliver a power as high as 300 W at 980 nm seem to be attractive for this scheme and motivate us to re-examine the idea in this paper.

2. Description of a TS-Probe

We envision measuring a divertor-leg plasma of 15 mm depth with a TS-probe as shown in Fig. 1.

It consists of a probe head, optical fibers, optical fiber feed-through, a laser diode, a polychromator, and lock-in amplifiers. These are described in details below.
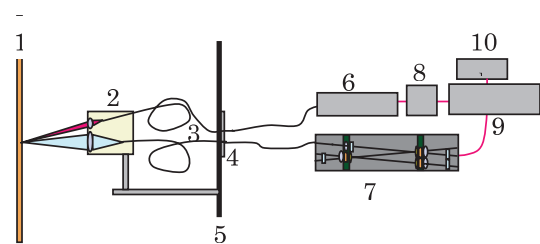
author's e-mail: narihara@nifs.ac.jp

Fig. 1 Schematic view of a TS-probe: 1. divertor-leg plasma; 2. TS-probe head; 3. optical fibers; 4. fiber feed-through; 5. vacuum chamber wall; 6. laser diode; 7. polychromator; 8. pulse generator; 9. lock-in amplifier; 10. data acquisition.
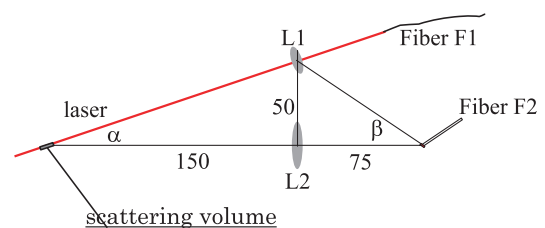

Fig. 2 Thomson scattering optics configuration. L1 and L2 are lenses.

(1) **Probe Head:** This is a compact optical bench on which laser delivery and light collection optics are firmly mounted. A key point is to collect as many TS photons as possible while keeping background plasma light at the smallest level. For this, it is important to form an image of the laser beam just on the surface of the light collection fiber with a slit of well-adjusted size. Figure 2 shows

the scattering configuration. In a simple geometry, the image of the oblique line (laser beam), which intersects L2's optical axis at an angle α, intersects the optical axis at β, which is related to α by $\tan\alpha/\tan\beta = m$. Here, $m = 75/150 = 1/2$ is the magnification.

An expanded view of the end of the optical fiber is shown in Fig. 3. The incident angle $\theta_1 = 90° - \beta$ is chosen so that light incident to the fiber is reflected as little as possible. If the laser beam, and hence the scattered light are properly polarized (p-waves), the reflectance at the fiber surface is less than 1 % for $45° < \theta_1 < 63°$ as shown in Fig. 4. Unfortunately, the fiber we planned on using depolarizes the propagating laser light even if it is initially polarized. The unpolarized light reflects from the surface of the fiber by 5 % on average for $45° < \theta_1 < 63°$, as shown in Fig. 4. We choose a central incident angle of $\theta_1 = 56°$; hence, $\beta = 34°$ and $\alpha = 17°$ for $m = 0.5$. The end of the fiber is cut at an angle of 56° so that centrally incident light propagates along the axis of the fiber after refraction. A slit 1 mm in length and 0.5 mm in width set at the obliquely cut surface of the fiber defines the scattering cylindrical volume $L = 3$ mm in length and $D = 1$ mm in diameter located at the waist point of the laser beam shaped by lens
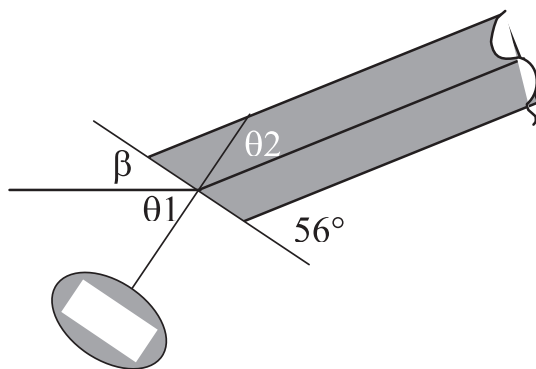

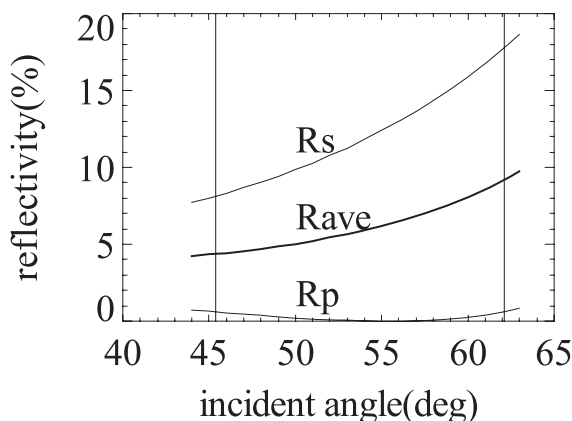Fig. 3 Magnified view of the optical fiber for collecting TS light.

Fig. 4 Reflectivity at the end surface of the fiber as a function of incident angle.

L1. L1 has a focal length $f = 34$ mm and diameter $\phi30$, which matches $NA = 0.22$ of fiber F1 with a core diameter of 0.5 mm.

Lens L2 has a focal length $f = 52$ mm and is 40 mm in diameter with a 34 mm × 40 mm square aperture, which matches the acceptance angle of fiber F2. The aperture gives a solid angle of $\Delta\Omega = 25$ msr. All optical components making up the TS probe are housed in a box $100 × 100 × 50$ mm^3 in size. The scattering configuration is similar to a 1/20 model of the Large Helical Device-TS (LHD-TS).

(2) **Optical Fibers**: Two optical fibers are used. F1 delivers high-power laser energy, and F2 transports the scattered light to a polychromator. Contrary to our intuition, it is reported that a step-index type optical fiber made of pure silica can transmit a high power density [2]; a 400 μm core diameter fiber can transmit 2000 W continuous wave (CW) light and a 1 MW/mm^2 light pulse width of < 1 ms. We found no progress in the transmittable power density in fibers in the past 13 years, probably indicating a mature state of the art. Considering an available laser diode of 300 W CW output, a core diameter of 500 μm is large enough for fiber F1. Lens L2 ($f = 52$ mm; 20 × 30 mm^2 aperture) focuses the scattered light onto the end surface of F2 at a 1-mm diameter cut at the Brewster angle.

Both fibers, set inside a vacuum chamber, are flexible enough that we can move the TS-probe head freely to a large extent. A simple metallic screen shields the fibers against plasma radiation that would otherwise heat them. Unavoidable exposure to hard x-rays and neutrons, if present, will result in a gradual drop in the transmission of the fibers and fluorescent emission from the body of the fibers. The latter problem will not be serious for the present case, in which a modulated laser beam is used. The former problem will be alleviated greatly by selecting a suitable fiber material and wavelength for the laser light (900-1100 nm) transmitted in the fiber. An increase in the temperature of the fibers, which may occur naturally or intentionally, will remove the defects introduced inside them.

(3) **Fiber Feed-Through:** This new product is useful for interfacing the fibers set inside and outside of a vacuum chamber. A commercially available fiber feed-through can be used for an ultra-high vacuum (UHV) environment of 10^{-10} mbar [3]. Durability against high power transmission must be investigated.

(4) **Light Sources:** The light source for TS must be intense enough to yield a sufficient signal and have a wavelength width narrow enough to discern Doppler broadening of the scattered spectrum due to thermal motion of plasma electrons. The allowable width ($\Delta\lambda$) depends on the minimum-measurable electron temperature T_{e_min} (eV), as follows: $\Delta\lambda/\lambda \ll T_{e\_min}^{0.5}/500$. For example, for $T_{e\_min} = 10$ eV,

$\Delta\lambda/\lambda \ll 6/1000$; and for $T_{e\_min} = 1$ eV, $\Delta\lambda/\lambda \ll 2/1000$. These values imply that it is not absolutely necessary to use lasers operating in a cavity, e.g., an Nd:YAG laser with $\Delta\lambda/\lambda \ll 10^{-6}$, as a TS light source. Laser diodes, which are widely used for pumping the laser rod and for industrial applications such as welding and cutting, seem suitable for the present purpose. Great progress in the power and beam quality of laser diodes has been made in the past decade. For example, LIMO GmbH produces a fiber-coupled laser diode module that delivers 980 nm, 350 W light from a 400 μm core fiber with $NA = 0.22$ [4]. The specified line width (FWHM) $\Delta\lambda < 8$ nm will allow T_e measurement to come down to $T_{e\_min} \sim 30$ eV, which is rather high for edge plasma measurement. Recently it was reported [5] that a Bragg grating stabilizes a diode laser to yield a power of 330 W from a fiber with $\Delta\lambda = 0.5$ nm line width at $\lambda = 967$ nm, allowing TS measurement down to a few eV. The above data are for CW operation. As described later, the laser diode should be modulated at a high frequency. Whether the ability to deliver high power degrades when the laser diode is used in a modulation mode is an open question.

(5) Polychromator: We will use a conventional three-filter polychromator. The principle of operation is based on the transmission and reflection characteristics of a combination of filters arranged to form a zigzag optical path. A key concern is to prevent stray light with the wavelength of the laser from entering the light detector, such as an avalanche photo diode (APD). In the case of the LHD-TS, each filter in the polychromator blocks the light at 1064 nm (the Nd: YAG laser wavelength) with a blocking factor of 10^5 (OD5). Even with this high blocking factor, some polychromators suffer from stray light. Considering that the power is as high as 300 W in the present case, the filters with a much higher OD level will be necessary. Setting a notch filter with OD ~4 at the laser wavelength at the exit of the fiber-lens may be a solution. In addition to the strong blocking, the steepness of the edge of the filters is important determining the lowest detectable T_e (T_{e_min}). Recently developed volume holographic optical filters [6] with narrow band-widths seem promising for solving this problem.

(6) Lock-in Amplifiers: These are used to pickup weak scattered signals modulated at frequency f_m in the presence of overwhelming background noise arising mainly from plasma light. In considering that the spectrum of plasma density fluctuation and the resultant plasma light fluctuation monotonically decreases down to the sub-MHz region, a reference frequency f_m higher than 1 MHz is favorable for reducing the noise contribution. A lock-in amplifier that operates at frequencies as high as 200 MHz is available: SR844 (Standard Research System) [7].

3. Signal-to-Noise Ratio

To assess the possible performance of the TS-probe described above, we estimate the accuracy of T_e and n_e values deduced from the outputs of the lock-in amplifiers. We consider a sheet-like divertor-leg plasma 15 mm deep with T_e less than 100 eV and n_e ranging from 10^{18} m^{-3} to 10^{20} m^{-3} with a modulated laser diode of $P_{LASER} = 300$ W and $\lambda_{LASER} = 980$ nm.

A backward TS spectrum is shown in Fig. 5 for various T_e, which are discriminated by three color channels with pass-bands B1 = [940, 960], B2 = [960, 970] and B3 = [970, 975] in nm unit. The light power fed to a polychromator is the sum of the scattered light P_{sct} plus the plasma radiation P_{rad}, which are given respectively as

$$P_{sct} = P_{LASER}n_e L(d^2\sigma/d\Omega d\lambda)\Delta\Omega\Delta\lambda$$
$$\approx 5.3 \times 10^{-19} P_{LASER}n_e L\Delta\Omega Sp(\lambda)d\lambda/\lambda_{LASER} \quad (1)$$

and

$$P_{rad} = j_v\Delta\nu\Delta V\Delta\Omega$$
$$\approx 1.5 \times 10^{-45} Z_{eff}n_e^2 T_e^{-1/2} G\Delta\Omega V_{obs}c\Delta\lambda/\lambda^2 . \quad (2)$$

Here, $Sp(\lambda)$ is the TS spectrum shown in Fig. 5, $\lambda_{LASER} = 980$ nm is the laser wavelength, j_v is the bremsstrahlung emissivity, Z_{eff} is the effective ion charge, G is the Gaunt factor enhanced ~5 times to take account of enhanced radiation due to recombination and line radiation, $V_{obs} \sim \pi D^2/4 \times 15 \sim 10$ mm^3 is the effective plasma volume that the collection optics see. The light power that falls in i-th filter's passband is incident to the i-th APD, inducing a current

$$j_i = \int d\lambda(P_{sct} + P_{rad})F_i(\lambda)\lambda/hc$$
$$\equiv j_{si} + j_{bi} . \quad (3)$$

Here, $F_i(\lambda)$ is the filter transmittance η_{FIL} times the quantum efficiency η_Q of the i-th channel: $F_i(\lambda) = \eta_{FIL}(\lambda)\eta_Q(\lambda)$.

We assume an idealized filter with $\eta_{FIL} = 0.9$ in the i-th passband and $\eta_{FIL} = 0$ otherwise. The responsivity
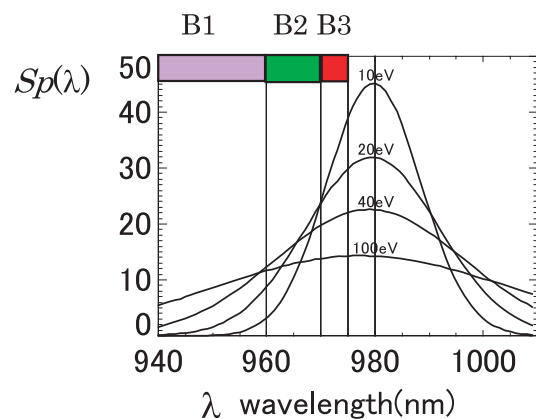
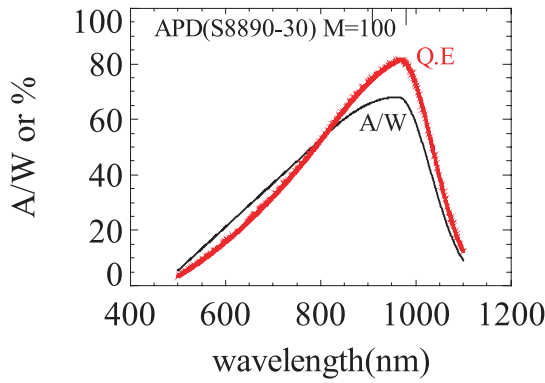Fig. 5 TS spectra for various T_e. Three color bands are indicated.

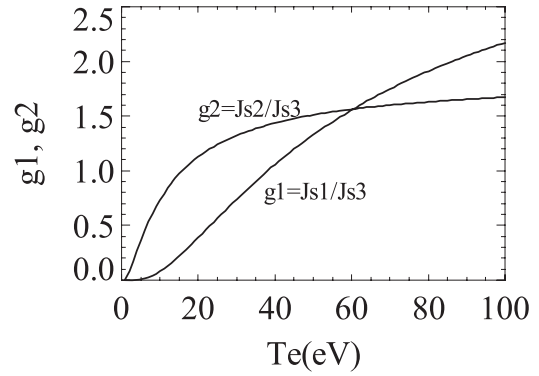Fig. 6 Responsivity and quantum efficiency of an APD (Hamamatsu S8890).

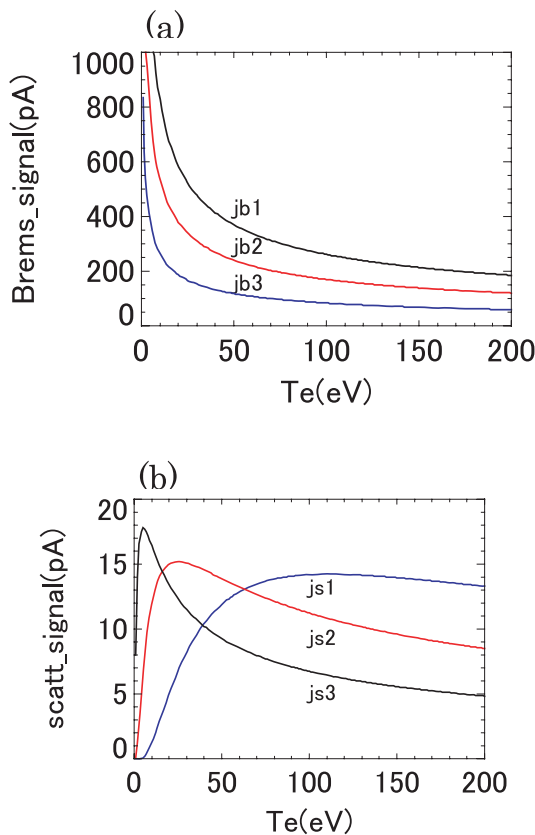Fig. 8 Two ratios among the TS signals from three-color channels.

Fig. 7 APD currents induced by (a) bremsstrahlung and (b) Thomson scatted light. $n_e = 10^{19} \, \text{m}^{-3}$.

(A/W) and its associated quantum efficiency η_Q (%) of an APD are shown in Fig. 6 as functions of wavelength, from which we reasonably set $\eta_Q = 0.75$ for the three passbands (940 nm $< \lambda <$ 975 nm). Figures 7 (a) and (b) show j_{bi} and j_{si} (i = 1-3) for a plasma with $n_e = 10^{19} \, \text{m}^{-3}$ as a function of T_e. We note that the scattering signals j_{si}; i = 1-3 are deeply buried in the plasma bremsstrahlung signals $\{j_{bi}; i = 1\text{-}3\}$. The APD outputs, which are proportional to $j_i = j_{si} + j_{bi}$ are fed to three lock-in amplifiers. A lock-in amplifier is a kind of Fourier analyzer if the reference in-

put is fed by a precise sinusoidal signal, which is also used to modulate the laser diode. The frequency spectrum of an APD's output is composed of two terms: a very narrow TS signal centered at the modulation frequency f_m and broadband noise generated mainly by shot noise. The current in the APD $j_i = j_{si} + j_{bi} + j_d$ generates the shot noise, whose power spectrum is given by

$$<i_n^2> = 2e j_i M^2 F_n(M) \Delta f_{APD} , \qquad (4)$$

where e is the elementary charge, $M \sim 100$ is the multiplication factor of the APDs, $F_n(M)$ is an excess noise factor, and Δf_{APD} is the bandwidth. Here, an inevitable dark current $j_d \sim 1 \, \text{nA}$ is added to the APD current. The appearance of $F_n(M)$ implies enhanced noise in the avalanche process in the APD [8–10]. $F_n(M)$ is dependent on the ratio of hole ionization to electron ionization. By suitable design and selection of the processing material, $F_n(M)$ can be less than 4 for $M = 100$ [10]. In this paper, we assume $F_n(M) = 10$. The RC-type integration time τ of a lock-in amplifier yields a spectrum width Δf_{BW} given by the relation $\Delta f_{BW} = 1/4\tau$. Then, the output of the lock-in amplifier is expressed as

$$y_i = j_{si} \pm (e j_i/2\tau)^{1/2} \equiv j_{si} \pm \delta y_i . \qquad (5)$$

Hence, however deeply the TS-light is buried in the plasma radiation, it is possible to pick up the TS signal by taking a long enough integration time.

With these data $\{y_i; i = 1\text{-}3\}$ we can estimate the errors in the deduced T_e and n_e by following the standard method. The two ratios $j_{s1}/j_{s3} \equiv g_1(T_e)$ and $j_{s2}/j_{s3} \equiv g_2(T_e)$ are functions of T_e alone, as shown in Fig. 8. Conversely, the observed ratios y_1/y_3 and y_2/y_3 give two T_e values: $y_1/y_3 = g_1(T_{e1})$ and $y_2/y_3 = g_2(T_{e2})$. The errors in T_{e1} and T_{e2} are calculated as

$$(\delta T_{e1})^2 = (g_1')^{-2}(\delta y_1^2/y_3^2 + y_1^2 \delta y_3^2/y_3^4) , \qquad (6)$$

$$(\delta T_{e2})^2 = (g_2')^{-2}(\delta y_2^2/y_3^2 + y_2^2 \delta y_3^2/y_3^4) , \qquad (7)$$

$$(\delta y_i)^2 = e j_i/2\tau \quad (i = 1\text{-}3) . \qquad (8)$$

With the variance $(\delta T_e)^2$ defined by

$$1/(\delta T_e)^2 = 1/(\delta T_{e1})^2 + 1/(\delta T_{e2})^2 , \qquad (9)$$

the most probable T_e is evaluated from the two ratios weighted by the reciprocal of the error in each ratio as

$$T_e = (T_{e1}/(\delta T_{e1})^2 + T_{e2}/(\delta T_{e2})^2)(\delta T_e)^2 . \qquad (10)$$

The error in n_e is obtained, for example, from y_3:

$$(\delta n_e/n_e)^2 = (\delta y_3/y_3)^2 + (\delta j_{s3}/\partial T_e)^2(\delta T_e)^2/j_{s3}^2 . \quad (11)$$

Figure 9 shows the relative errors in T_e and n_e, $\sqrt{\delta(T_e)^2}/T_e$ and $\sqrt{(\delta n_e)^2}/n_e$, as a function of T_e for four combinations of parameters:

(a) $n_e = 10^{19}$ m^{-3}, $P_{LASER} = 300$ W and $\tau = 0.1$ s;
(b) $n_e = 10^{19}$ m^{-3}, $P_{LASER} = 100$ W and $\tau = 0.5$ s;
(c) $n_e = 10^{20}$ m^{-3}, $P_{LASER} = 300$ W and $\tau = 0.05$ s;
(d) $n_e = 10^{18}$ m^{-3}, $P_{LASER} = 300$ W and $\tau = 1$ s.

For each n_e and P_{LASER} combination, τ is chosen to give relative errors less than 10 % for a wide range of T_e. From these figures we can say that: (a) a plasma with $n_e \geq 10^{19}$ m^{-3} can be measured with time resolution of 0.1 s; (b) a smaller laser power of $P_{LASER} = 100$ W results in a less favorable signal-to-noise ratio in y_i, which in turn requires an integration time longer than 0.5 s to yield reasonable data quality; (c) for a plasma ten times denser, $n_e = 10^{20}$ m^{-3}, an integration time of 0.05 s is necessary for the same $P_{LASER} = 300$ W; (d) a lower-density plasma of $n_e = 10^{18}$m^{-3} can be measured with $P_{LASER} = 300$ W by a much longer integration time, up to 1 s. We can see that $\sqrt{(\delta n_e)^2}/n_e < \sqrt{(\delta T_e)^2}/T_e$ for all the cases. This may be explained by the fact that T_e is deduced from the ratios among $\{y_i\}$, while n_e is deduced from $\{y_i\}$ directly. In practice, however, taking into account the error arising from a calibration process, the error in n_e is usually larger than the error in T_e. The filter passband combination shown in Fig. 5 is not optimized to give the best performance. However, it is considered that the result shown in Fig. 9 will not change much with adjustment to the filter passband combination, but rather shows general features.

4. Discussion

We re-examined the feasibility of a fiber-based TS-probe 13 years after an initial proposal [1]. During this period, we observed great progress in high-power laser diodes, which may be used as a light source. A newly developed fiber feed-through is adopted in the design as a convenient optical component. It was shown that a currently available laser diode of 300 W can yield 10 % accuracy in T_e and n_e data for a plasma of $n_e \sim 10^{19}$ m^{-3} with an integration time of 0.1 s. This may be useful for measuring slowly changing or steady-state plasma discharges.

Now we discuss possible ways of improving this performance, i.e., lowering errors and shortening the integra-
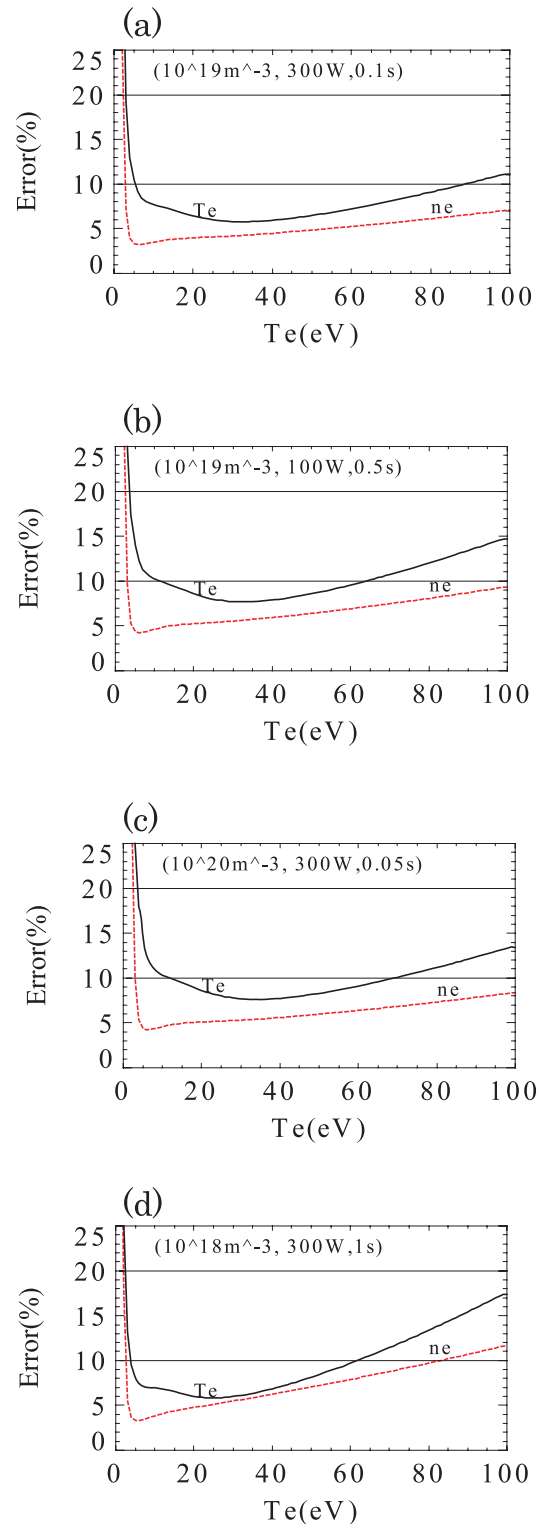
Fig. 9 $\sqrt{(\delta T_e)^2}/T_e$ and $\sqrt{(\delta n_e)^2}/n_e$ for: (a) $n_e = 10^{19}$ m^{-3}, $P_{LASER} = 300$ W and $\tau = 0.1$ s; (b) $n_e = 10^{19}$ m^{-3}, $P_{LASER} = 100$ W, and $\tau = 0.5$ s; (c) $n_e = 10^{20}$ m^{-3}, $P_{LASER} = 300$ W and $\tau = 0.05$ s; (d) $n_e = 10^{18}$ m^{-3}, $P_{LASER} = 300$ W, and $\tau = 1$ s.

tion time. In the above analyses, noise arises predominantly from the shot noise induced by plasma light enhanced by the avalanche process. An enhancement factor
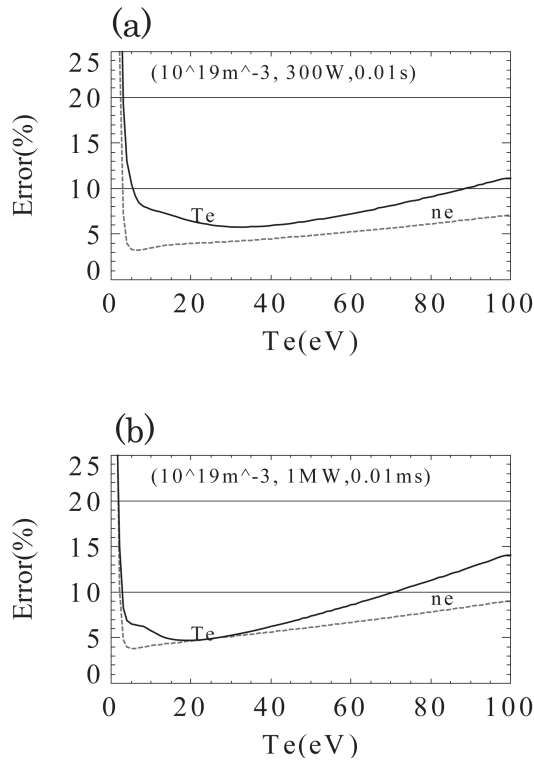
(a)

(b)

Fig. 10 (a) $\sqrt{(\delta T_e)^2}/T_e$ and $\sqrt{(\delta n_e)^2}/n_e$ for P_{LASER} = 300 W, n_e = 10^{19} m^{-3}, and τ = 0.01 s without enhanced noise in the APD. (b) $\sqrt{(\delta T_e)^2}/T_e$ and $\sqrt{(\delta n_e)^2}/n_e$ for P_{LASER} = 1 MW, n_e = 10^{19} m^{-3} and τ = 0.01 ms.

$F_n(M)$ = 10 is supposed in this paper. If APD noise were unenhanced, that is, $F_m(M)$ = 1, the noise power spectrum in Eq. (5) would be reduced appreciably. In this case, the errors in T_e and n_e are much reduced, and an integration time of 0.01 s is long enough to yield accurate data, as shown in Fig. 10 (a).

For this reason, developing less noisy photo detectors is desirable [10]. The second way of improving performance is to raise the probe light power. The key element of the TS-probe is intense light transmission in a fiber. A ϕ1.2 fiber, which is still flexible, can transmit CW light of 2 kW and 1 MW pulses with duration less than 1 ms. If a 1 MW laser of 0.01 ms pulse width is available, it will provide enough accuracy with τ = 0.01 ms, as shown in Fig. 10 (b). The feasibility of such high-power light from a laser diode is beyond the scope of present paper. A solid-state laser such as a Nd: YAG laser pumped by a laser diode may yield such light, but it will be much less efficient, and hence, expensive. The third way of improving performance is to reduce the V_{obs} as much as possible. The assumed V_{obs} ~10 mm^3 is determined by the waist size (ϕ1 mm) of the laser beam at the scattering position, which is largely dependent on the diameter and *NA* of the laser-transmitting fiber. A smaller diameter and smaller *NA* are favorable for reducing the beam size. If a laser diode powered by a flexible cable can be mounted on the TS-probe head, the beam size at the focal point may be reduced to ϕ0.1, thus lowering V_{obs} and P_{rad} by two orders of magnitude, if the beam quality is good enough.

We showed the feasibility of the TS-probe, but to realize it in practice, we must solve some technical issues, such as: (1) how to modulate 300 W laser output power at a high frequency of MHz, (2) how to dump the high-power laser energy of 300 W without damaging the neighboring structures, and (3) how to lower stray light to a level at which the weak scattered light can be discriminated.

[1] K. Narihara *et al.*, Fusion Eng. Des. **34-35**, 67 (1997).
[2] Diaguide, Mitsubishi-cable Catalog 2000. 07 (in Japanese).
[3] http://www.lewvac.co.uk.
[4] http://www.LIMO.de.
[5] Laser Focus World Japan **8**, 52 (2008).
[6] C. Moser, L. Ho, E. Maye and F. Havermeyer, J. Phys. D: Appl. Phys. **41**, 224003 (2008).
[7] http://www.Thinkers.com/products/SR844.htm.
[8] A. van der Ziel, *Noise*, Prentice-Hall, Inc, 1954.
[9] R. J. McIntyre, IEEE Trans. Electron Devices **ED-13**, 164 (1966).
[10] 'The Avalanche Photodiode Catalog', Advanced Photonix, Inc.